ELSEVIER

Computational Materials Science 18 (2000) 283–294

COMPUTATIONAL MATERIALS SCIENCE

www.elsevier.com/locate/commatsci

# Strain-induced Kirkendall mixing at semiconductor interfaces

K. Nordlund *, J. Nord, J. Frantz, J. Keinonen

*Accelerator Laboratory, University of Helsinki, P.O. Box 43, Helsinki 00014, Finland*

Received 3 February 2000; accepted 22 March 2000

**Abstract**

We use molecular dynamics computer simulations to study the damage production by collision cascades at Si/Ge and AlAs/GaAs and InAs/GaAs interfaces. For the arsenide systems we find that present interatomic potentials have troubles in describing even the basic elastic and melting properties. We report parameter refinements which give a significantly better description of these properties. Our results for collision cascades at strained semiconductor interfaces show a strong asymmetry in the distribution of vacancies and impurities produced at the interface. The effect is explained as a strain-induced effect analogous to the classical Kirkendall effect. We also show that although the chemical composition of compound semiconductors does not strongly affect the overall evolution of collision cascades, the composition may in some cases have a significant effect on the final distribution of defects. 

*PACS:* 61.82.Fk; 61.72.Ji; 68.35.Dv

*Keywords:* Irradiation; Defects; Interfaces; Semiconductors; Strain; Interfacial mixing

## 1. Introduction

Ion-irradiation is nowadays used in several different ways in semiconductor manufacturing. Ion-implantation has for a long time been used to introduce dopants into silicon [1], but more recently ion beams have also become commercially interesting for uses such as exfoliation (“Smart Cut”) for the production of silicon-on-insulator wafers [1] [2,3] and implantation through the gate of transistors to achieve better transistor performance [4]. Implantation is also used in the manufacturing of compound semiconductor components [5].

The use of these novel techniques also poses a challenge for controlling defect behaviour during the implantation and subsequent annealing stages. While the overall process of damage production and annealing has been extensively studied and is reasonably well understood in silicon [6], effects in compound semiconductors and at interfaces between two materials have been much less examined. Experiments on AlAs/GaAs systems show in fact that significant asymmetries in the damage production can exist at semiconductor interfaces [7]. Furthermore, recent molecular dynamic (MD) simulations indicate that dramatic asymmetries may exist in the distribution of

* Corresponding author. Tel.: +358-9-19140007; fax: +358-9-19140042.

*E-mail address:* kai.nordlund@helsinki.fi (K. Nordlund).

[1] Smart Cut is a registered trademark of SOITEC.

0927-0256/00/$ - see front matter 
PII: S0927-0256(00)00107-5

vacancies during irradiation of metal interfaces [8]. If similar interface effects would be present in the semiconductors, it could have a significant effect on the damage annealing in multilayer structures and semiconductor components. For instance, if the number of interstitials and vacancies would not be equal in one part of a component then full damage recombination could be inhibited.

The collision cascades induced by ion-irradiation behave quite differently in semiconductors and metals. In pure metals, a cascade forms a large liquid-like zone, which, however, recrystallizes almost perfectly as the cascade region cools down [9,10]. Interstitials are formed at the outskirts of the cascade, whereas vacancies are pushed towards the cell center by the recrystallization front [11]. This ''vacancy push'' effect can lead to an asymmetry in the defect distribution at interfaces [8]. In semiconductors, by contrast, the open crystal structure largely prevents instant recrystallization of damage at low temperatures. Instead, the liquid pockets formed in cascades tend to form an amorphous zone in the crystal [10]. Due to this difference in behaviour, it is not clear whether the interface effect seen in metals could also be present in semiconductors. Although there is very little recrystallization in semiconductors, there might still be a vacancy push-like effect in the amorphous zone. On the other hand, the large strain frequently associated with semiconductor interfaces might also give rise to asymmetries in damage production at interfaces.

To examine these issues, we have simulated collision cascades at Si/Ge, AlAs/GaAs and InAs/GaAs interfaces. Since these systems have quite different properties with respect to the melting point and interface strain, they should provide a fairly comprehensive view of what kinds of irradiation interface effects can be expected to be present at common semiconductor interfaces.

This paper is organized as follows. In the next section we discuss at some length problems of the interatomic potentials in arsenide systems, and remedies to them. In Section 2, we present the simulation results, and in the end we compare the results to those obtained in metals and experiments.

## 2. Simulation method

### 2.1. Collision cascades

To study interface effects induced by ion-irradiation, we simulated collision cascades in simulation cells containing two different materials. The cells had periodic boundaries in three dimensions, and were divided in the middle into two zones with a (1 0 0) or (1 1 1) crystal interface plane. The number of atoms was between 25 and 64 atoms per eV of the initial recoil energy for 400 eV–2 keV cascades, and about 90 atoms per eV for 5 keV cascades. These number of atoms were chosen such that they are large enough to prevent any energetic recoil from reaching the boundaries of the simulation cell.

The cascade simulations were started at an initial temperature of 0 K, and the cells were cooled down towards 0 K at the cell borders using Berendsen pressure control [12]. This ensured that any defect reactions occurring in the simulations are a result of the cascade, rather than thermal defect migration or annealing. In all the cases, the cell was equilibrated to an average zero pressure separately in the three-dimensions prior to initiation of the cascade. This leads to the two materials having strains of opposite sign in the two-dimensions parallel to the interface plane, and zero pressure in the direction perpendicular to it.

Energetic recoils were initiated in the atom planes closest to the interface on both sides of it, by giving a recoil velocity in a random direction in the interface plane. We also used recoils started outside the interface and directed towards it, and obtained qualitatively similar results as for the interface recoils. Due to the difficulty of placing recoils outside the interface, so that the nuclear deposited energy is evenly divided on both sides of the interface, quantitative interpretation of these results is difficult, and we do not report the results. The recoil energies used ranged from 400 eV to 5 keV. In the compound semiconductor materials equal numbers of recoils were started from the sites of both of the material constituents. No significant differences depending on from what site the recoil was started were noted in the cascade results.

For the Si/Ge interfaces we usually used (1 0 0) interfaces, although (1 1 1) interfaces were also tested. For AlAs/GaAs and InAs/GaAs we used (1 1 1) interfaces because in these materials a (1 0 0) interface has an As atom plane in the middle which cannot be uniquely assigned to "belong" to either of the two materials.

Defects (vacancies, interstitials and antisites) were recognized using Voronoy polyhedra centered on atom positions in a perfect crystal prior to the onset of the cascade. Although this method is in no way a unique way to recognize and label defects, we have shown earlier that other methods give qualitatively similar results [10]. Note that if an interstitial atom is on the site of an atom of the opposite type, in our definition it will be counted both as an antisite atom and an interstitial. Also, because of the complex shape of the Voronoy polyhedra an interstitial atom right at an interface may in a few cases be counted to belong to an interstitial on the other side of the interface.

To enable recognition of possible interface effects on damage production, we also simulated cascades in Si, Ge, AlAs, GaAs and InAs without the presence of an interface. To find out whether the chemical composition of the arsenides affects the cascade development, we also created "homogeneous" AlAs, GaAs and InAs. Taking GaAs as an example, this means that we made the Ga–Ga and As–As interaction potential equal to the Ga–As one, creating a material with the equilibrium properties of real GaAs, but no chemical difference between the constituent atoms. This operation is straightforward in Tersoff-like potentials, where it can be done simply by setting all elemental potential parameters $p_{\mathrm{As–As}}$ and $p_{\mathrm{Ga–Ga}}$ equal to the compound parameter $p_{\mathrm{Ga–As}}$. Here $p$ denotes any of the potential parameters [13,14]. The atom masses were still held at their original values to keep the ballistic behaviour similar. We will label these artificial materials h-AlAs, h-GaAs and h-InAs.

Except for the special features mentioned above, the cascade simulation and damage analysis methods used were the same as those described in Ref. [10].

Physically, these simulation conditions correspond to collision cascades initiated by recoils of a passing high-energy ion close to a semiconductor interface. While some of the interfaces (such as Si/Ge and InAs/GaAs) have lattice mismatches which are not observed in macroscopic samples, the difference to the maximal mismatches observed in equilibrium is not more than $\sim$2% [1]. Furthermore, at dislocated semiconductor interfaces the local stresses might well be comparable to those in our simulations. Since our interest here is primarily in recognizing qualitative features in the cascade development which may occur at interfaces, use of interface structures with somewhat too large strains are in fact useful in that possible interface effects are easier to recognize.

### 2.2. Interatomic potentials

During ion-irradiation effects of solids, large deformations of the lattice and even melting can occur in the solid. Hence for simulations of such effects it is important to use interatomic potentials which can describe lattice deformations, bond breaking and melting. The elastic moduli and melting properties of the potential can be used as a first-order measure of whether these effects are adequately described.

For Si and Ge numerous interatomic potentials exist, and have been extensively tested [15]. We chose to use the Stillinger–Weber [16] (SW) and Tersoff III [17] models for Si. For Ge we used a modification of the Stillinger–Weber parametrization by Ding and Andersen [10,18] and Tersoff [13,14] models. All of these models reproduce fairly the three elastic constants of cubic systems. The Stillinger–Weber models also have good melting properties [10]. Provided a realistic repulsive potential has been joined to the models, the models are also known to give a reasonable description of irradiation effects [10,19]. The Si–Ge cross potentials were obtained by a straightforward averaging of the Si and Ge parameters [13,14,20].

For compound semiconductors, the situation is far less developed. Although a few potentials exist which describe properties close to equilibrium well [21,22] these cannot be used to describe irradiation effects since they are clearly unsuitable for describing large lattice distortions.

Smith [23], Sayed et al. [24] and Ashu et al. [25] have developed potential models in the Tersoff functional form, which purport to describe properties far from equilibrium in AlAs, GaAs and InAs. Since we have recently found problems with both the Smith and Sayed GaAs models [26], we examined these models in greater detail, and report the results here.

The elasticity and melting values obtained by us are given in Table 1. The elastic constants were obtained by calculating Young's modulus $Y$ and the elastic modulus $Y_{[111],\|}$ [27] using MD simulations with periodic boundaries in all dimensions. This ensured that the simulations gave $C_{44}$ values which account correctly for internal relaxations in the zincblende lattice [28]. The melting point was calculated using the method of finding the equilibrium temperature for co-existing liquid and solid phases at zero pressure [29].

The original Sayed AlAs and GaAs models both showed a rapid segregation of the elemental components of the materials on melting, whence we do not give a melting point value for them in Table 1. For AlAs we found that the original Sayed parameter values [24] gave quite reasonable elastic and melting properties after setting $\lambda_3 = 0$.

Table 1
Elastic and melting properties of the Tersoff-based interatomic potentials tested in this study[a]

| Material and model | $C_{11}$ | $C_{12}$ | $C_{44}$ | $T_{\text{melt}}$ |
|---|---|---|---|---|
| AlAs, Sayed[b] | 1203 | 570 | 683 | – |
| AlAs, present work | 1203 | 570 | 683 | $2200 \pm 200$ |
| GaAs, Smith[c] | 800 | 800 | $\lesssim 10$ | $1250 \pm 100$ |
| GaAs, Sayed[b] | 1190 | 530 | 690 | – |
| GaAs, present work | 1190 | 530 | 690 | $1050 \pm 100$ |
| InAs, Ashu[d] | 680 | 680 | $\lesssim 10$ | $1200 \pm 100$ |
| InAs, present work | 836 | 453 | 396 | $1100 \pm 100$ |
| AlAs, expt. | 1202 | 570 | 589 | 2013 |
| GaAs, expt. | 1180 | 540 | 590 | 1510 |
| InAs, expt. | 833 | 453 | 396 | 1215 |

[a] The experimental values of the elastic constants are from Ref. [37]. Note that the elastic constant calculations allow for internal relaxation in the lattice; a calculation of $C_{44}$ without internal relaxation gives in some cases very different results. The AlAs and GaAs potentials of the current work are as the original Sayed potentials, except that the $\lambda_3$ parameter has been set to zero. The InAs potential has been completely refitted.

[b] Ref. [24].

[c] Ref. [38].

[d] Ref. [25].

For the Smith GaAs potential we found that the two elastic constants $C_{11}$ and $C_{12}$ had practically identical values, leading to a Young's modulus $Y$ of practically zero. Similarly, the value of $C_{44}$ is also very small (due to numerical inaccuracies, we only determined an upper limit for $C_{44}$). The reason to these problems is the very weak angular term in the Smith potential [24,26]. Even though we found that the value of $C_{44}^{(0)}$, the shear modulus in absence of internal strain [28], is quite reasonable, the weak angular dependence leads to an internal strain parameter $\zeta$ [28] of almost exactly 1. Hence the physically measured elastic constant $C_{44}$ will also be much smaller than $C_{44}^{(0)}$. Since vanishingly small values of $Y$ and $C_{44}$ lead to very unrealistic deformation properties, we did not use the Smith potential in further work. The Sayed GaAs potential [24] gave fairly reasonable behaviour after setting $\lambda_3 = 0$ [26,30].

For InAs, we found that the potential of Ashu et al. [25] did not even give the right equilibrium lattice constant, and that the angular term was far too weak to describe deformation properties properly. Hence we refitted all the potential parameters for the In–As interaction. This was done by starting from the Ga–As Sayed parameters, and modifying them until a fit which gave about the right interatomic separation, elastic moduli and melting point, ensuring that no parameter value was drastically modified from the original value. While this procedure gives an InAs model which we believe is adequate for modeling strain and melting for InAs in the zincblende structure, it is clear that it has limited transferability.

These modified potentials should thus meet the basic requirements for an ion-irradiation potential in that the elasticity properties and short-lived liquid states are described at least fairly reasonably. In particular, they are suitable for the purposes of the present paper, namely *qualitatively* examining whether melting or strain effects at interfaces can affect collision cascades in semiconductors. But because of the poor physical motivation in the original potential fits, it is clear

Table 2
Parameter values for the Tersoff-like potentials used in this study. The notation is as in Refs. [13,14] [a]

| | In–Ga | In–In | Al–Ga | Al–Al | Al–As | In–As | As–As | Ga–As | Ga–Ga |
|---|---|---|---|---|---|---|---|---|---|
| $n$ | 3.43739 | 3.40223 | 4.59759 | 6.086505 | 4.047579 | 0.7561694 | 0.60879133 | 6.31741 | 3.4729041 |
| $c$ | 0.0801587 | 0.084215 | 0.0755633 | 0.074836 | 1.449752 | 5.172421 | 5.273131 | 1.226302 | 0.07629773 |
| $d$ | 19.5277 | 19.2626 | 19.6825 | 19.569127 | 0.828713 | 1.665967 | 0.75102662 | 0.790396 | 19.796474 |
| $h$ | 7.26805 | 7.39228 | 3.24333 | −0.659266 | −0.520946 | −0.5413316 | 0.15292354 | −0.518489 | 7.1459174 |
| $\beta$ | 0.705241 | 2.10871 | 0.273372 | 0.316846 | 0.330946 | 0.3186402 | 0.00748809 | 0.357192 | 0.23586237 |
| $\lambda$ | 2.5616 | 2.6159 | 2.54688 | 2.585337 | 2.8090295 | 2.597556 | 2.384132239 | 2.82809263 | 2.50842747 |
| $\mu$ | 1.58314 | 1.68117 | 1.20913 | 0.927442 | 1.5582295 | 1.422429 | 1.7287263 | 1.72301158 | 1.490824 |
| $A$ | 1719.7 | 2975.54 | 699.824 | 492.7659 | 2307.8794 | 1968.295443 | 1571.86084 | 2543.29720 | 993.888094 |
| $B$ | 221.557 | 360.61 | 55.9917 | 23.031117 | 219.1396 | 266.571631 | 546.4316579 | 314.459660 | 136.123032 |
| $R$ | 3.4 | 3.5 | 3.4 | 3.4 | 3.4 | 3.5 | 3.4 | 3.4 | 3.4 |
| $S$ | 3.6 | 3.7 | 3.6 | 3.6 | 3.6 | 3.7 | 3.6 | 3.6 | 3.6 |

[a] The AlAs and GaAs system parameters are the same as those of Sayed et al. [24] except for the value of the $\lambda_3$ parameter, and the In–As parameters are new fits by us. For completeness we list also the parameter values which have not been modified by us. The parameter $\lambda_3$ is not used in any of our potentials.

that the exact defect production numbers and defect structures cannot be considered to be reliable. To examine defects in detail, better classical potentials, or an electronic structure calculation model, clearly is needed.

The parameter values used by us are listed in Table 2 , but we emphasize that we do not recommend transferring the present potentials to other kinds of problems without extensive testing of their suitability.

In addition to the Tersoff-based models described above, Conrad and Scheerschmidt have recently introduced a Si and GaAs model where hopping matrix elements from a tight-binding model have been used in the angular term of a Tersoff-like potential [31], while other potential parameters have been fit to Si and GaAs properties. While this idea is attractive in that tight-binding parameters that exist for a wide range of materials, it does involve a "double fitting" in the sense that the tight-binding parameters already fits to physical properties, and on top of this a second fit is made in formulating the Tersoff-like classical potential. Hence great care should be taken in the final fit to ensure that artifacts do not arise. In tests of the Conrad GaAs model we found that melting GaAs collapses into a state lower than −3.6 eV/atom in potential energy, much less than the equilibrium value of −3.25 eV/atom. Tests of melting pure Ga and As within the Conrad model revealed that both elements also collapse into states with much lower cohesive energies than the experimental values, showing that the model is quite unsuitable for describing any far-from equilibrium state of Ga, As and GaAs.

## 3. Results

### 3.1. Effect of interface on damage production

To find whether the presence of an interface affects the total numbers of defects produced, we list in Table 3 the total numbers of Frenkel pairs

Table 3
Production of Frenkel pairs $N_{FP}$, number of displaced atoms $N_{displ}$ and total atom relocation $R^2_{tot}$ (proportional to the ion beam mixing) in 1 keV cascades in Si, Ge, AlAs, GaAs and InAs, and in events right at Si/Ge, AlAs/GaAs and InAs/GaAs interfaces[a]

| | $N_{FP}$ | $N_{displ}$ | $R^2_{tot}$ |
|---|---|---|---|
| Ge | 18.0 ± 2.8 | 137 ± 15 | 2830 ± 110 |
| Si | 10.2 ± 0.8 | 77 ± 8 | 2160 ± 240 |
| Si/Ge | 16.6 ± 1.6 | 115 ± 7 | 2630 ± 90 |
| AlAs | 11.2 ± 0.4 | 23 ± 1 | 1820 ± 130 |
| GaAs | 14.1 ± 0.5 | 29 ± 1 | 1770 ± 210 |
| InAs | 17.0 ± 1.0 | 41 ± 3 | 1930 ± 290 |
| AlAs/GaAs | 12.0 ± 0.7 | 26 ± 1 | 1960 ± 170 |
| InAs/GaAs | 16.6 ± 0.9 | 35 ± 1 | 1440 ± 70 |

[a] The numbers are averages for equal numbers of recoils of all atom types in each system. The original Stillinger–Weber (SW) and modified Ge SW models were used for these results (see text).

produced $N_{FP}$, the number of displaced atoms $N_{displ}$ and the square of the total atom relocation distances $R^2_{tot}$ [32] for 1 keV cascades in all the materials studies (by a "1 keV cascade" or "1 keV event", we mean a collision cascade initiated by a 1 keV recoiling atom, and similarly for other energies). For the interface cases Si/Ge, AlAs/GaAs and InAs/GaAs all the quantities are simply summed over the whole simulation cell.

The results show that in almost all the cases, the evaluated quantities at interfaces fall between those in the corresponding single-component simulations. The only quantity where there is a significant deviation to this is the atom relocation at the InAs/GaAs interface. However, due to the large variation in the mixing values and this can be due to a statistical fluctuation. For AlAs/GaAs the results are essentially in the middle between the AlAs and GaAs values. For Si/Ge and InAs/GaAs, the results at the interface are closer to the larger value of the two constituent materials. This behaviour can be understood in terms of the lattice mismatches: for AlAs/GaAs the lattice mismatch is less than 0.2%, whereas for Si/Ge it is about 4% and for InAs/GaAs about 7%. Hence, the AlAs/GaAs interface will not be affected by the strain, whereas in the Si/Ge and InAs/GaAs systems the large strains at the interface will slightly increase the damage production and number of relocated atoms.

However, considering the very large strains at the Si/Ge and InAs/GaAs interfaces, it is remarkable that the damage production increases only marginally at the interface, even though a considerable amount of energy is transferred to the lattice. The most likely reason is that the cascade energy density still remains fairly low due to the open nature of the zincblende crystal structure [10], and the strong covalent bonding makes it difficult to produce dislocations relieving the strain.

### 3.2. Asymmetries in damage production at interface

To find out whether asymmetries in the damage production exist at interfaces, we calculated the number of defects produced separately on both sides of the interface. The location of the interface was defined as the midpoint between the atom planes closest to the interface.

For the Si/Ge interface systems the results are listed in Tables 4 and 5. Table 4 shows results for 1 keV cascades modeled by SW potentials giving the right melting point both for Si and Ge, and Table 5 results for 2 keV cascades at the Si/Ge interface for *different* interatomic potentials.

Comparison of the results for the 1 keV Si/Ge interface with those in Si and Ge (Table 4) shows that while the total damage production is indeed about the same, the damage is not distributed evenly in the interface case. There are significantly more vacancies on the Ge than Si side of the interface. This is explained by the distribution of impurity atoms, i.e. atoms which have crossed the initial location of the interface during the collision cascade. There are significantly more Ge impurities on the Si side of the interface than Si impurities on the Ge side. The distribution of interstitials, however, is the same on both sides of the interface. This effect is similar to the inverse Kirkendall mixing effect observed earlier at metal interfaces [8] in that the vacancy and impurity distributions are asymmetric, but the interstitial distribution is not.

The reason to the symmetric distribution of interstitials in both cases is that most interstitials are produced by high-energy ballistic relocation of

Table 4
Results for 1 keV cascades in Si and Ge and at a (1 0 0) Si/Ge interface[a]

| | Si side | | | Ge side | | |
|---|---|---|---|---|---|---|
| | $N_i$ | $N_v$ | $N_{imp.}$ | $N_i$ | $N_v$ | $N_{imp.}$ |
| Si | $10.2 \pm 0.8$ | $10.2 \pm 0.8$ | – | – | – | – |
| Ge | – | – | – | $17.6 \pm 3.0$ | $18.0 \pm 2.8$ | – |
| Si/Ge | $7.8 \pm 1.0$ | $4.5 \pm 1.0$ | $7.5 \pm 1.1$ | $8.1 \pm 1.1$ | $12.1 \pm 1.3$ | $3.9 \pm 0.8$ |

[a] The table gives the number of interstitials $N_i$, vacancies $N_v$ and impurities $N_{imp.}$ for Si and Ge, and separately on the Si and Ge sides of the (1 0 0) Si/Ge interface. The numbers are averages for equal numbers of recoils of all atom types in each system.

Table 5
Distribution of vacancies and impurities in 2 keV cascades at Si/Ge interfaces modeled by different Si and Ge interatomic potentials[a]

| Potential model | Si side | | Ge side | |
|---|---|---|---|---|
| | $N_v$ | $N_{imp.}$ | $N_v$ | $N_{imp.}$ |
| SW | $13.4 \pm 1.7$ | $15 \pm 2$ | $18.5 \pm 2$ | $10.5 \pm 1.8$ |
| Unmodified SW | $14.1 \pm 1.9$ | $7.6 \pm 1.5$ | $5.5 \pm 0.9$ | $4.2 \pm 0.8$ |
| SW (1 1 1) | $8.7 \pm 1.2$ | $14 \pm 3$ | $22 \pm 5$ | $9.3 \pm 1.9$ |
| Tersoff (1 1 1) | $29 \pm 2$ | $5.9 \pm 1.5$ | $12 \pm 3$ | $3.7 \pm 0.7$ |
| a-SiGe | – | $24 \pm 4$ | – | $12 \pm 3$ |

[a] The model notation is as follows: "SW" is the original Stillinger–Weber parametrization for Si [16] and our modified Stillinger–Weber parametrization giving the right melting point of Ge. "Unmodified SW" is the unmodified parametrizations for both Si [16] and Ge [18]. "Tersoff" are results for the Tersoff Si and Ge potentials [14]. (1 1 1) denotes events which were started in a cell with a (1 1 1) rather than a (1 0 0) interface between the materials, and "a-Si/a-Ge" denotes a simulation cell of amorphous Si and Ge. The numbers are averages for equal numbers of recoils of all atom types in each system.

atoms, which is not affected much by the presence of an interface [10]. However, the reason to the vacancy and impurity asymmetry is not as clear. In the metals the effect is explained by pushing of the vacancies in the liquid zone of the cascade onto the side of the material with the lower melting point, which also leads to a pushing of atoms to the other side of the interface.

Since Ge has a lower melting point than Si, this mechanism could also explain the effect at the Si/Ge interface. To test the idea, we simulated cascades with other Si and Ge interatomic potentials, many of which had unrealistic melting properties. These results are shown in Table 5, and the different models described in the caption. The vacancy distribution is similar in all the cases except for the Tersoff and unmodified SW potentials, where there are more vacancies on the Si side. This is because in these models Ge has too stiff bonding and a much too high melting point, reducing the damage production significantly [10].

Even though the distribution of vacancies across the interface is thus affected by the melting point of the materials, the distribution of impurities is not. The same asymmetry in the distribution of impurities is present in every case, even for the unrealistic Tersoff and unmodified Stillinger–Weber Ge models [10]. In every case, there are more impurities on the Si than Ge side of the interface. The presence of the same impurity asymmetry in all the cases shows that the effect cannot be due to a melting point difference of the materials. The asymmetry is even present at an interface between amorphous Si and Ge, showing that the effect is not due to the crystal structure either.

The remaining explanation, which we think is the only plausible one consistent with all the cases, is that the effect is induced by the strain at the interface. This strain is present in all the different models. The Ge atoms at the interface are subject to a strong local compressive strain, and the Si atoms subject to a tensile strain. The collision cascade can induce a relaxation of both strains by displacing some Ge atoms over the interface onto the Si side. Since the number of atoms must be conserved, some atoms will hence be missing on the other side of the interface, showing up as vacancies in the damage calculation.

The defect distribution is illustrated in Fig. 1, which shows the distribution of impurity atoms on both sides of the interface for 2 keV Si/Ge events.

Since in this case (contrary to the case in metals) a flow of atoms induces a flow of vacancies in the opposite direction, this effect is analogous to the classical Kirkendall effect [33,34] [2]. Although the driving force behind the effect is of course quite different in the current case, due to the similarity in the flows this effect can be considered as a strain-induced Kirkendall mixing effect.

The energy dependence of the effect is illustrated in Fig. 2. The asymmetry in the defect production is clearly present at all the energies examined. The vacancy and impurity numbers raise about linearly up to 2 keV, but the number of

[2] For discussion see e.g. [35].

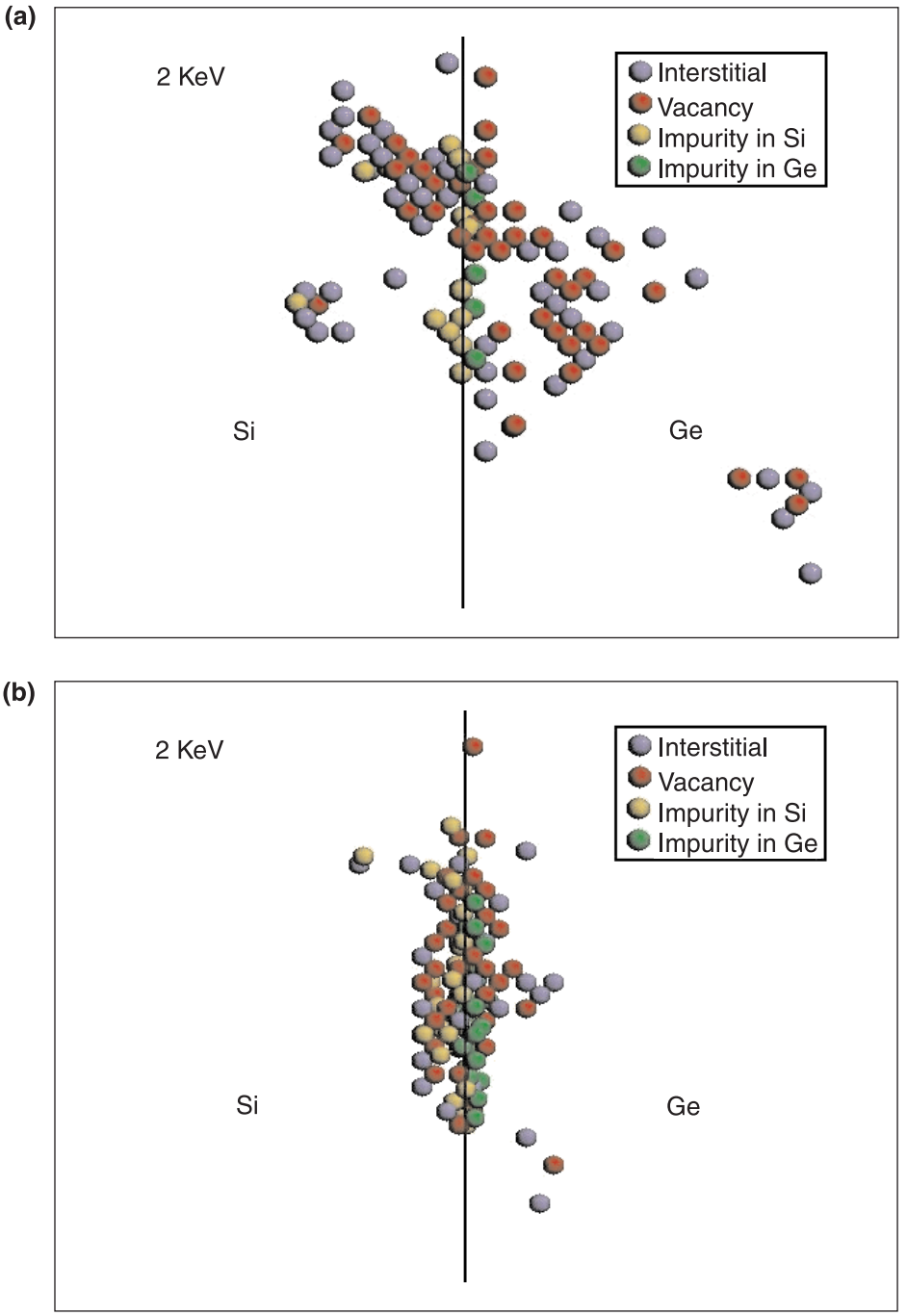


Fig. 1. Final distribution of damage in two different 2 keV cascades started in the (1 0 0) interface plane of a Si/Ge interface. Note that in both events there are more impurities on the Si than Ge side of the interface after the cascade.

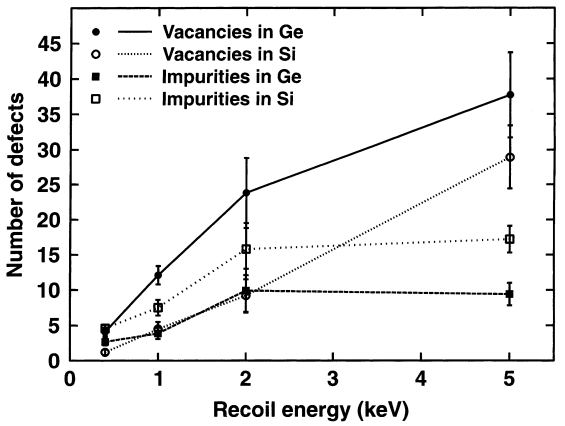


Fig. 2. Energy dependence of the production of defects in cascades initiated close to the (1 0 0) interface plane in Si/Ge systems.

impurities levels off after that. The reason is simply that around 5 keV the cascade becomes so extended in space that most atom displacements occur far from the interface, and hence cannot produce any impurities. Still, it is interesting to note that the asymmetry in the impurity numbers still exists even at 5 keV, showing that the effect may be significant even during higher energy irradiation.

As a further test of whether the effect is strain-induced, we also simulated AlAs/GaAs and InAs/GaAs interfaces. Since the lattice mismatch is practically zero in the former case, and about 7% in the latter, the effect should be present only at the InAs/GaAs interface provided that our proposition is right. The results in Table 6 confirm that this is indeed the case. For the AlAs/GaAs interface the number of atoms which have crossed the interface $N_{cross}$ is the same within the uncertainties, whereas for the InAs/GaAs interface there is a clear difference. To avoid counting antisites formed by recoils moving only on one side of the interface, we use the quantity $N_{cross}$ rather than the number of impurities here.

Quantitatively, however, the results here are quite different from those at the Si/Ge interface at 1 keV (Table 4); the number of atoms which have crossed the interface is roughly a factor of 4 smaller than in the Si/Ge system. The most likely reason to this is that the elastic constants in InAs are almost a factor of 2 smaller than those in Si and Ge, reducing the strength of the elastic force pushing atoms over the interface. It is also possible that deficiencies in the potentials play a role in the smaller quantitative effect.

Another factor reducing the relocation of atoms over the interface is the chemical composition of the element. Table 6 also gives results for an interface between "homogeneous" InAs and GaAs, which shows a somewhat larger atom relocation than that in the "real" materials. This shows that in the real material, the atom relocation over the interface is suppressed by chemical effects.

### 3.3. Chemical effects in compound semiconductor cascades

The results of cascades in compound semiconductors allow us to gauge whether chemical effects (that is, the presence of two chemically different

Table 6
Results for 1 keV cascades in AlAs, GaAs, InAs and at the (1 1 1) AlAs/GaAs and InAs/GaAs interfaces[a]

| | AlAs/InAs side | | | GaAs side | | |
|---|---|---|---|---|---|---|
| | $N_i$ | $N_v$ | $N_{cross}$ | $N_i$ | $N_v$ | $N_{cross}$ |
| AlAs | 11.1 ± 0.4 | 11.2 ± 0.4 | – | – | – | – |
| GaAs | – | – | – | 14.1 ± 0.5 | 14.1 ± 0.5 | – |
| InAs | 16.8 ± 0.9 | 17.0 ± 1.0 | – | – | – | – |
| AlAs/GaAs | 6.4 ± 0.5 | 6.7 ± 0.6 | 1.0 ± 0.2 | 5.6 ± 0.4 | 5.3 ± 0.4 | 1.1 ± 0.2 |
| InAs/GaAs | 6.7 ± 0.5 | 7.6 ± 0.6 | 1.7 ± 0.2 | 10.0 ± 0.6 | 9.1 ± 0.7 | 0.9 ± 0.2 |
| h-InAs/h-GaAs | 7.8 ± 0.6 | 9.2 ± 0.9 | 2.5 ± 0.3 | 10.3 ± 0.5 | 8.9 ± 0.7 | 1.1 ± 0.2 |

[a] The table gives the number of interstitials $N_i$, vacancies $N_v$ and atoms which have crossed the interface $N_{cross}$ for the single-component materials, and separately on the two sides of the (1 1 1) interfaces. The numbers are averages for equal numbers of recoils of all atom types in each system.

Table 7
Cascade results for 1 keV cascades in AlAs, GaAs and InAs, and their artificial "homogeneous" counterparts[a]

| | $N_{FP}$ | $N_{antis}$ | $N_{displ}$ |
|---|---|---|---|
| AlAs | $11.2 \pm 0.4$ | $9.8 \pm 0.8$ | $23.4 \pm 0.9$ |
| GaAs | $14.1 \pm 0.5$ | $11.6 \pm 0.9$ | $29.0 \pm 0.8$ |
| InAs | $17.0 \pm 1.0$ | $13.1 \pm 0.9$ | $41.3 \pm 2.9$ |
| h-AlAs | $9.6 \pm 0.6$ | $10.6 \pm 0.8$ | $20.9 \pm 1.0$ |
| h-GaAs | $12.6 \pm 0.7$ | $12.6 \pm 0.9$ | $25.9 \pm 1.3$ |
| h-InAs | $19.7 \pm 0.9$ | $23.0 \pm 1.3$ | $43.5 \pm 1.2$ |

[a] Listed is the number of Frenkel pairs $N_{FP}$ produced, number of antisite defects $N_{antis}$, and number of displaced atoms $N_{displ}$. The numbers are averages for equal numbers of recoils of all atom types in each system.

atom types) could affect the cascade evolution significantly. We compare the results in cascades in a "real" material with those in an artificial "homogeneous" material. Since the atoms in the latter materials differ only in their mass, but not in their interactions, this comparison unambiguously show whether the nature of the component interactions affects the cascade development.

The results in Table 7 show that overall there are no major chemical effects in these 1 keV cascades. The production of Frenkel pairs $N_{FP}$ and number of displaced atoms $N_{displ}$ are almost the same in the "real" and "homogeneous" materials within the uncertainties in all the cases. Although there are small differences, it is difficult to judge whether they are statistically significant, and in any case they are less than about 20%.

The one instance where a large chemical effect exists is in the number of antisites $N_{antis}$ produced in InAs. In "real" InAs the value is about 13, whereas in the "homogeneous" InAs it is about 23. This indicates that antisite production is clearly suppressed by the compound structure of the material. The reason that this effect is not observed in AlAs and GaAs is most likely that the number of displaced atoms $N_{displ}$ is much higher in InAs. This, in turn, is due to the heavy mass of In and the elastic softness of the material. Test simulations with an artificial InAs structure, where the mass of the In atoms was set equal to the mass of As atoms indicated that roughly half of the effect was due to the higher mass of In, and the other half due to the elastic softness.

Since cascades at higher energies in the zinc-blende crystal structure break-up in subcascades at energies around 2–5 keV, not very far from the present energy used, our results show that chemical effects dramatically affecting the evolution of cascades cannot be expected to be present in common III–V compounds, during any irradiation conditions producing damage in collision cascades.

The InAs results show, however, that the resulting damage distribution may be strongly affected by the chemical composition of the material, but with the present uncertainties of the interatomic potentials we cannot state this with higher certainty.

## 4. Discussion

The results presented in this paper show that some interface effects can clearly be present at strained semiconductor interfaces. The effects can be relatively large at energies $\sim$1 keV, but diminish in relative magnitude going to energies around 5 keV. This is in contrast to dense metals, where very pronounced effects can still be present at 5 keV [8] and probably even at higher energies. The reason to the difference is that the open crystal structure leads to fairly dilute cascades in semiconductors [10], thus reducing the relative magnitude of the interface effects as most of the cascade is not located at the interface.

Another difference between metals and semiconductors is the mechanism leading to asymmetries in the damage production at interfaces. Whereas in close-packed metals the dominant effect appears to be a recrystallization front pushing vacancies on one side of the interface, in semiconductors we do not find this effect. This can again be understood based on the general nature of the cascade development: In semiconductors most of the disordered zone produced in the cascades remains in an amorphous state [19,36], whence there is no driving force for defect motion during the cooling down stage of the cascade.

In semiconductors we found that a strain effect can lead to an asymmetry in defect distribution at

an interface. While the strain in the systems we used in this study were somewhat larger than those in most common epitaxial systems, the qualitative features can still be expected to be the same in strained systems. Furthermore, even at incoherent interfaces where misfit dislocation relieve strain, large local atom-level strains are present and effects similar to those discussed in this paper could be an issue. Due to the sensitivity of the electrical properties of semiconductors to small defect concentrations, even a small relative effect could have important consequences.

To date, one of the most extensive set of experimental studies of radiation effects at interfaces have been the studies of $Al_xGa_{1-x}As/GaAs$ interfaces by Robertson et al., who did indeed find asymmetries in the damage production [7]. Since the strain associated with these interfaces is quite low, however, it is not likely that this effect is related to that found in the present work.

We also found indications that although the overall cascade development (as measured for instance by the number of displaced atoms) is not affected by the chemical composition of a compound semiconductor, in some cases the final damage distribution may be significantly affected even at fairly high energies like 1 keV. At very low energies close to the displacement threshold energy even more significant effects can of course be present.

## 5. Conclusions

To conclude, by simulating collision cascades in Si, Ge, AlAs, GaAs, and InAs and at interfaces formed between these materials, we have explored to what extent interface and chemical effects may affect the outcome of collision cascades. During the course of the work, we identified several problems with existing arsenide potentials, and propose here remedies solving the most acute problems in simulations of far-from-equilibrium effects. Our cascade results show that while the overall amount of damage produced in energetic cascades is not strongly affected by the presence of an interface, the distribution of damage on two sides of an interface can be strongly asymmetric due to a strain-induced Kirkendall-like effect. The results also indicate that at least in some compound semiconductor materials, chemical effects may clearly suppress antisite production and the distribution of damage over the interface.

## Acknowledgements

We thank Prof. R.S. Averback for enlightening discussions about the role of the strain on the cascades and Drs. K. Albe and A. Kuronen for useful discussions regarding interatomic potentials and the calculation of elastic constants. We are also grateful to Dr. D. Conrad for providing his molecular dynamics simulation code for our use. The research was supported by the Academy of Finland under projects No. 44215 and 46788. Generous grants of computer time at the Center for Scientific Computing in Espoo, Finland are gratefully acknowledged.

## References

[1] J.W. Mayer, S.S. Lau, Electronic Materials Science for Integrated Circuits in Si and GaAs, MacMillan, New York, 1990.
[2] M. Bister, J. Hirvonen, J. Räisänen, A. Anttila, Radiat. Eff. 59 (1982) 199.
[3] M. Bruel, B. Aspar, A.-J. Auberton-Herve, Jpn. J. Appl. Phys. 36 (1997) 1636.
[4] P.A. Stolk, Y.Y. Ponomarev, J. Schmitz, A.C.M.C. van Brandenburg, R. Roes, A.H. Montree, P.H. Woerlee, Nucl. Instr. and Meth. B 148 (1999) 242.
[5] M. Hong, J. Kow, A.R. Kortan, J.P. Mannaerts, A.M. Sergent, Science 283 (1999) 1897.
[6] M. Chason et al., J. Appl. Phys. 81 (1997) 6513.
[7] B.A. Turkot, B.W. Lagow, I.M. Robertson, D.V. Forbes, J.J. Coleman, L.E. Rehn, P.M. Baldo, J. Appl. Phys. 80 (1996) 4366.
[8] K. Nordlund, R.S. Averback, Phys. Rev. B 59 (1999) 20.
[9] T. Diaz de la Rubia, R.S. Averback, R. Benedek, W.E. King, Phys. Rev. Lett. 59 (1987) 1930.
[10] K. Nordlund, M. Ghaly, R.S. Averback, M. Caturla, T. Diaz de la Rubia, J. Tarus, Phys. Rev. B 57 (1998) 7556.
[11] K. Nordlund, R.S. Averback, Phys. Rev. B 56 (1997) 2421.
[12] H.J.C. Berendsen, J.P.M. Postma, W.F. van Gunsteren, A. DiNola, J.R. Haak, J. Chem. Phys. 81 (1984) 3684.
[13] J. Tersoff, Phys. Rev. B 39 (1989) 5566.
[14] J. Tersoff, Phys. Rev. B 41 (1990) 3248.
[15] H. Balamane, T. Halicioglu, W.A. Tiller, Phys. Rev. B. 46 (1992) 2250.

[16] F.H. Stillinger, T.A. Weber, Phys. Rev. B 31 (1985) 5262.
[17] J. Tersoff, Phys. Rev. B 38 (1988) 9902.
[18] K. Ding, H.C. Andersen, Phys. Rev. B 34 (1986) 6987.
[19] M.-J. Caturla, L.A.M.T. Diaz de la Rubia, G.H. Gilmer, Phys. Rev. B 54 (1996) 16683.
[20] Z.Q. Wang, D. Stroud, Phys. Rev. B 38 (1988) 1384.
[21] T.I.K.E. Khor, S. Das Sarma, J. Vac. Sci. Technol. B 8 (1990) 669.
[22] M.C. Schabel, J.L. Martins, Phys. Rev. B. 43 (1991) 11873.
[23] R. Smith, Nucl. Instr. and Meth. B 67 (1992) 335.
[24] M. Sayed, J.H. Jefferson, A.B. Walker, A.G. Gullis, Nucl. Instr. and Meth. B 102 (1995) 232.
[25] P.A. Ashu, J.H. Jefferson, A.G. Cullis, W.E. Hagston, C.R. Whitehouse, J. Cryst. Growth 150 (1995) 176.
[26] K. Nordlund, A. Kuronen, Nucl. Instr. and Meth. B 159 (1999) 183.
[27] P. Heino, H. Häkkinen, K. Kaski, Europhys. Lett. 41 (1998) 273.
[28] O.H. Nielsen, R.M. Martin, Phys. Rev. B 32 (1985) 3792.
[29] J.R. Morris, C.Z. Wang, K.M. Ho, C.T. Chan, Phys. Rev. B 49 (1994) 3109.
[30] A. Kuronen, J. Tarus, K. Nordlund, Nucl. Instr. and Meth. B 153 (1999) 209.
[31] D. Conrad, K. Scheerschmidt, Phys. Rev. B 58 (1998) 4538.
[32] K. Nordlund, M. Ghaly, R.S. Averback, J. Appl. Phys. 83 (1998) 1238.
[33] A. Smigelskas, E. Kirkendall, Trans. AIME 171 (1947) 130.
[34] L. Darken, Trans. AIME 174 (1948) 184.
[35] P.G. Shewmon, Diffusion in Solids, McGraw-Hill, New York, 1963 (Chapter 4).
[36] T. Diaz de la Rubia, G.H. Gilmer, Phys. Rev. Lett. 74 (1995) 2507.
[37] D. Bimberg et al., in: K.-H. Hellwege (Ed.), LANDOLT-BÖRNSTEIN Numerical Data and Functional Relationships in Science and Technology, vol. III17/a, Springer, Berlin, 1982.
[38] R. Smith, B. King, K. Beardmore, Radiat. Eff. Def. Sol. 141 (1997) 425.